J|A|C|S
COMMUNICATIONS

Published on Web 11/25/2003

$^1H-^1H$ Dipolar Couplings Provide a Unique Probe of RNA Backbone Structure

Emeric Miclet,[†] Erin O'Neil-Cabello,[†,‡] Edward P. Nikonowicz,[‡] David Live,[§] and Ad Bax*[,†]

Laboratory of Chemical Physics, NIDDK, National Institutes of Health, Bethesda, Maryland 20892-0520, Department of Biochemistry and Cell Biology, Rice University, POB 1892, Houston, Texas 77251, and Department of Biochemistry, University of Minnesota, Minneapolis, Minnesota 55455

Received October 1, 2003; E-mail: bax@nih.gov

The ability to weakly align a macromolecule in solution relative to an external magnetic field, usually by means of a dilute lyotropic liquid crystalline medium, makes it possible to obtain direct information on the orientation of internuclear bond vectors from the residual internuclear dipolar couplings (RDCs) by NMR.[1−3] So far, most practical applications have focused on the measurement of one-bond interactions, particularly those for the backbone $^{15}N-^1H$ and $^{13}C^\alpha-^1H^\alpha$ groups in proteins and also on other one-bond interactions such as $^{13}C^\alpha-^{13}C'$ and couplings across the peptide bond ($^{13}C'-^{15}N$). Measurements of fixed-distance dipolar interactions for nuclei separated by two or three bonds also have proven to be useful in this regard.[4−6] More recently, attention has focused on measurement of ^1H-^1H RDCs[7−9] which, despite the variable internuclear distance, can also easily be integrated in structure determination protocols.[10]

Remarkably, the $^1H-^1H$ coupling between geminal methylene protons is often more difficult to measure accurately. These protons frequently have a complex multiplet shape and fall in a crowded region of the ^1H spectrum. This made it essentially impossible to measure these couplings for the C5′ and many of the C2′ sites in a palindromic DNA dodecamer,[11] for example. However, measurement of the individual $^{13}C-^1H_A$ and $^{13}C-^1H_B$ interactions in methylene groups has been reported for a drug bound to a perdeuterated protein, where spectral complexity is greatly reduced.[7] A clever alternate approach measures simultaneously the $^{13}C-^1H_A$, $^{13}C-^1H_B$, and $^1H_A-^1H_B$ dipolar interactions but for practical reasons is not easily applied to side chain methylene groups in proteins or to nucleic acids.[12]

Here, we demonstrate a simple two-dimensional NMR experiment that yields accurate measurement of both the sum of the $^{13}C-^1H_A$ and $^{13}C-^1H_B$ couplings and the geminal $^1H_A-^1H_B$ coupling, even in regions of the NMR spectrum that are often considered inaccessible due to spectral crowding. The experiment narrows the line width in the ^1H dimension by suppressing part of the $^1H-^1H$ multiplet, thereby enhancing resolution.

The pulse scheme used for measurement of $^2J_{HH}$ and $^2D_{HH}$ couplings is shown in Figure 1. ^1H magnetization is initially transferred to ^{13}C by means of an INEPT transfer, and subsequently either the downfield or upfield component of the ^{13}C triplet is selected by the $90°_x$ ^{13}C pulse (time point *a*), the final pulse of a so-called S^3E element.[13] The choice of the RF phase ϕ_1 is such that the ^{13}C Boltzmann component of the magnetization is co-added to the INEPT-transferred component selected by S^3E, thereby partially offsetting the loss of signal from one of the two $^{13}C-\{^1H\}$ multiplet components, observed in regular ^1H-coupled HSQC spectra. At the end of the constant-time evolution period, the *x* component of ^{13}C magnetization, $C_x + 4C_xH_{1z}H_{2z} \pm 2(C_xH_{1z} + C_xH_{2z})$, is stored along the *z*-axis (time *b*), where the "+" sign refers to the case where the upfield ^{13}C triplet component is selected, and the "−" sign to the downfield component. The subsequent "Rance−Kay" style transfer[14] converts these terms into $\pm(H_{1x}c_{12}s_{21} + H_{2x}c_{11}s_{22}) - 2H_{1x}H_{2z}s_{11}s_{12}c_{21}s_{22} - 2H_{2x}H_{1z}s_{11}s_{12}s_{21}c_{22} - 2H_{1z}H_{2x}c_{21}s_{22} - 2H_{1x}H_{2z}s_{21}c_{22}$, where $s_{ij} = \sin(\pi J_{CHj}\tau_i)$ and $c_{ij} = \cos(\pi J_{CHj}\tau_i)$, where τ_i designates τ_1 or τ_2 in Figure 1.

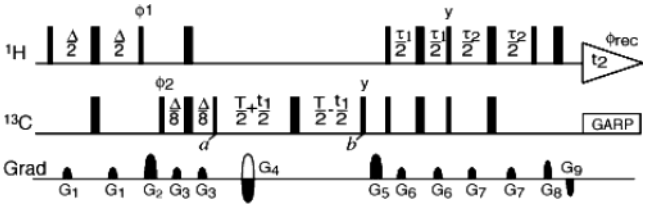

Figure 1. Pulse scheme of the CH_2-S^3E HSQC experiment. Narrow and wide bars indicate nonselective 90 and 180° pulses, respectively. Unless specified, pulse phases are *x*. Delay durations: $\Delta = 1/(2JCH) = 3.35$ ms; $\tau_1 = 1.48$ ms; $\tau_2 = 2.03$ ms. For selection of the upfield ^{13}C component: $\phi_1 = y$; $\phi_2 = (135°, -45°)$; $\phi_{rec} = (x,-x)$. The experiment is recorded in the echo−antiecho manner: for each t_1 increment, two FIDs are acquired, one with G_4 inverted, and stored separately. For selecting the ^{13}C downfield component: $\phi_1 = -y$; $\phi_2 = (225°, 45°)$; $\phi_{rec} = (x,-x)$. Field gradients are sine-bell shaped with durations $G_{1,...,9}$ of 1, 2, 0.25, 2, 2, 0.2, 0.3, 0.35, 0.153 ms, amplitudes of 10, 18, 12, 30, 20, 10, 12, 30, 30 G/cm, and directions *x*, *xy*, *y*, *z*, *xy*, *x*, *y*, *z*, *z*.

For suitably chosen durations of the delays τ_1 and τ_2, where $c_{12}s_{21} \approx s_{11}s_{12}c_{21}s_{22} + s_{21}c_{22}$, the above summation corresponds to $A(H_{1x} \pm 2H_{1x}H_{2z}) + A(H_{2x} \pm 2H_{2x}H_{1z})$, which represent the upfield ("−" sign for $J_{H1H2} < 0$) and downfield ("+" sign) components of the $H_1-\{H_2\}$ and $H_2-\{H_1\}$ doublets. Thus, with suitably chosen τ_1 and τ_2 values, the Rance−Kay element selectively converts the downfield CH_2 triplet component into the upfield components of the $H_1-\{H_2\}$ and $H_2-\{H_1\}$ doublets. As shown in Supporting Information, the selectivity of this transfer is relatively insensitive to the precise value of J_{CH}, and undesired transfers are suppressed by more than 10-fold for up to ±30 Hz deviations in J_{CH} when selecting $\tau_{1,2}$ durations for optimal S/N ($\tau_1 = 0.21/J_{CH}$; $\tau_2 = 0.30/J_{CH}$; $A = 0.65$ in the above expression). For shorter durations of $\tau_{1,2}$, even more robust suppression of unwanted transfers can be obtained, albeit at lower S/N. For example, for $\tau_1 = 0.125/J_{CH}$ and $\tau_2 = 0.2/J_{CH}$, calculations indicate $A = 0.55$, and 50-fold suppression is obtained for variations of up to ±40 Hz from the nominal J_{CH}. Calculations and simulations[15] indicate that higher sensitivity can be obtained when the $90°_y$ purge pulse (time point *b*) and gradient G5 are omitted in Figure 1 (Supporting Information), but this makes suppression of the unwanted multiplet component more sensitive to inhomogeneity of the radio frequency field, and this option is therefore not used.

The above transfer from one $^{13}C-\{^1H\}$ triplet component to a single $^1H-\{^1H\}$ component is conceptually similar to the so-called ST2-PT transfer from $^{15}N-\{^1H\}$ to $^1H-\{^{15}N\}$ doublet components

[†] National Institutes of Health.
[‡] Rice University.
[§] University of Minnesota.

10.1021/ja0388212 CCC: $25.00

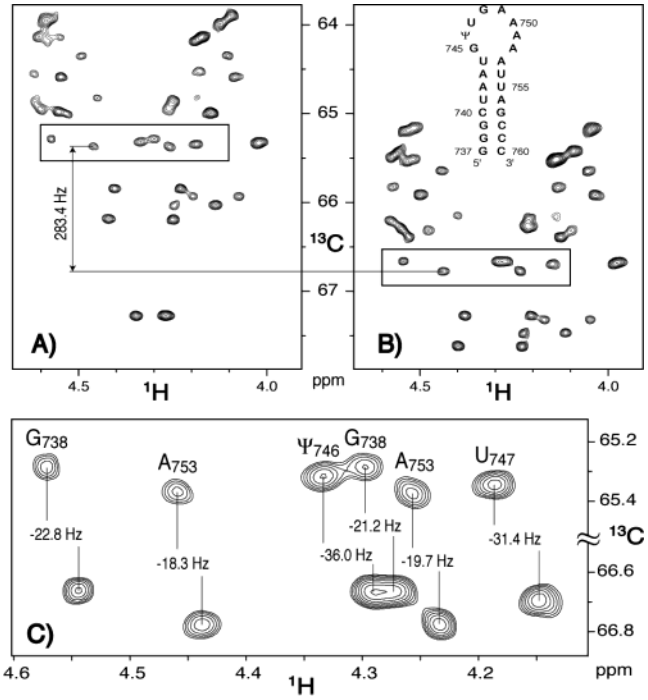

Figure 2. C5′ regions of the 800 MHz CH_2-S^3E [^{13}C,^{1}H] HSQC spectra of the uniformly ^{13}C-enriched stem-loop RNA oligomer, in 22 mg/mL Pf1. Sample conditions: 1.9 mM RNA oligomer, 10 mM NaCl, 10 mM phosphate, pH 6.8, 0.05 mM EDTA, 99% D_2O, 25 °C. The spectra containing (A) the ^{13}C-upfield and (B) the downfield components of the ^{13}C5′ triplets were acquired in an interleaved manner, with acquisition times of 25 (t_1) and 85 (t_2) ms, 8 scans per FID. (C) Composite of expanded regions of spectra (A) and (B). Horizontal and vertical relative displacements correspond to $^2J_{H5'-H5''} + {}^2D_{H5'-H5''}$ and $^1J_{C5'-H5'} + {}^1J_{C5'-H5''} + {}^1D_{C5'-H5'} + {}^1D_{C5'-H5''}$, respectively.

used in TROSY experiments[16] and also bears similarity to the "SPITZE-HSQC" transfer experiment, which relies on heteronuclear Hartmann−Hahn transfer.[12] Although the total amount of magnetization transferred in the experiment of Figure 1 is about 2-fold smaller than that in an optimized Rance−Kay transfer, all magnetization is present in half of the ^{1}H−{^{1}H} doublet. Therefore, in cases where geminal $^2J_{HH} + {}^2D_{HH}$ couplings are resolved, the experiment yields S/N comparable to the normal case, where delay durations are chosen to optimize net transfer.

The experiment is carried out at 800 MHz ^{1}H frequency, on a sample containing 1.9 mM of a uniformly ^{13}C-enriched RNA stem-loop oligomer, mimicking nucleotides 737−760 of *E. coli* 23S ribosomal RNA, and modified to contain ψ_{746}. The sample also contains 22 mg/mL liquid crystalline Pf1, which functions to impose weak alignment relative to the magnetic field on the solute RNA structure.[17] Figure 2 demonstrates the quality of the CH_2-S^3E−HSQC spectra, obtained with a constant-time (CT) duration of $1/J_{CC} \approx 25$ ms. Better ^{13}C resolution, at a cost of lower S/N, can be obtained for CT = 50 ms. The up- and downfield ^{13}C−{^{1}H} multiplet components are separated into Figures 2A and 2B. Their relative displacement in the ^{13}C dimension corresponds to $^1J_{CH1} + {}^1J_{CH2} + {}^1D_{CH1} + {}^1D_{CH2}$. The expansion shown in Figure 2C highlights the relative displacement of multiplet components in the ^{1}H dimension, which corresponds to $^2J_{H1H2} + {}^2D_{H1H2}$. Data measured under isotropic conditions indicate a relatively uniform $^2J_{H1H2}$ value of −11 Hz. With the exception of the 5′-terminal C5′H_2 group, all methylene groups also show quite uniform $^1J_{CH1} + {}^1J_{CH2} = 298 \pm 1$ Hz values (Supporting Information). Note that in the absence of overlap, two independent measures for each splitting are obtained from H5′ and H5″, yielding information on their reproducibility and permitting averaging of these values to improve accuracy. In virtually all cases, pairwise differences were smaller than 1 Hz.

In the aligned state, highly negative values are observed for $^2J_{H1H2} + {}^2D_{H1H2}$, corresponding to negative $^2D_{H1H2}$ values for all nucleotides. The *z*-axis of the alignment tensor is approximately parallel to the helical axis of the stem region of this structure. Negative values therefore indicate a H5′−H5″ vector pointing in the same direction. This is expected for the A-form helical stem region, but it is remarkable that the same feature is observed for all eight loop nucleotides too.

Our results indicate that dipolar couplings for methylene groups in ^{13}C-enriched biomolecules can be measured at high accuracy, even in spectral regions that frequently are considered intractable. In oligonucleotides, this provides important experimental restraints for the frequently ill-determined backbone torsion angles; in proteins the same experiment yields invaluable information on side chain conformation and dynamics. The experiment also yields $^1D_{C5'-H5'} + {}^1D_{C5'-H5''}$ values, which function as important complementary restraints in structure calculation,[18] and analogously the $^1D_{C2'-H2'} + {}^1D_{C2'-H2''}$ and $^1D_{H2'-H2''}$ values in DNA.

Acknowledgment. We thank David Fushman for help with computer simulations, Jerome Boisbouvier for discussions, and the Association pour la Recherche sur le Cancer for financial support (to E.M.). David Live was on leave at NIDCR/NIH.

Supporting Information Available: Plots of transfer efficiency as a function of τ_1 and τ_2 for the purged and Rance−Kay versions, plots of the ratio of the largest unwanted transfer and the selected transfer as a function of mismatch in J_{CH}, and a table with scalar and dipolar H5′−H5″ couplings, observed in the RNA stem-loop. This material is available free of charge via the Internet at http://pubs.acs.org.

References

(1) Gayathri, C.; Bothner-by, A. A.; van Zijl, P. C. M.; Maclean, C. *Chem. Phys. Lett.* **1982**, *87*, 192−196.
(2) Tolman, J. R.; Flanagan, J. M.; Kennedy, M. A.; Prestegard, J. H. *Proc. Natl. Acad. Sci. U.S.A.* **1995**, *92*, 9279−9283.
(3) Tjandra, N.; Bax, A. *Science* **1997**, *278*, 1111−1114.
(4) Yang, D. W.; Venters, R. A.; Mueller, G. A.; Choy, W. Y.; Kay, L. E. *J. Biomol. NMR* **1999**, *14*, 333−343.
(5) Yan, J. L.; Corpora, T.; Pradhan, P.; Bushweller, J. H. *J. Biomol. NMR* **2002**, *22*, 9−20.
(6) Zidek, L.; Wu, H. H.; Feigon, J.; Sklenar, V. *J. Biomol. NMR* **2001**, *21*, 153−160.
(7) Olejniczak, E. T.; Meadows, R. P.; Wang, H.; Cai, M. L.; Nettesheim, D. G.; Fesik, S. W. *J. Am. Chem. Soc.* **1999**, *121*, 9249−9250.
(8) Tian, F.; Fowler, C. A.; Zartler, E. R.; Jenney, F. A.; Adams, M. W.; Prestegard, J. H. *J. Biomol. NMR* **2000**, *18*, 23−31.
(9) Wu, Z. R.; Bax, A. *J. Am. Chem. Soc.* **2002**, *124*, 9672−9673.
(10) Tjandra, N.; Marquardt, J.; Clore, G. M. *J. Magn. Reson.* **2000**, *142*, 393−396.
(11) Wu, Z.; Delaglio, F.; Tjandra, N.; Zhurkin, V. B.; Bax, A. *J. Biomol. NMR* **2003**, *26*, 297−315.
(12) Carlomagno, T.; Peti, W.; Griesinger, C. *J. Biomol. NMR* **2000**, *17*, 99−109.
(13) Meissner, A.; Duus, J. O.; Sorensen, O. W. *J. Biomol. NMR* **1997**, *10*, 89−94.
(14) Kay, L. E.; Keifer, P.; Saarinen, T. *J. Am. Chem. Soc.* **1992**, *114*, 10663−10665.
(15) Nicholas, P.; Fushman, D.; Ruchinsky, V.; Cowburn, D. *J. Magn. Reson.* **2000**, *145*, 262−275.
(16) Pervushin, K. V.; Wider, G.; Wuthrich, K. *J. Biomol. NMR* **1998**, *12*, 345−348.
(17) Hansen, M. R.; Mueller, L.; Pardi, A. *Nature Struct. Biol.* **1998**, *5*, 1065−1074.
(18) Ottiger, M.; Delaglio, F.; Marquardt, J. L.; Tjandra, N.; Bax, A. *J. Magn. Reson.* **1998**, *134*, 365−369.

JA0388212